30. Gattinoni L, Powell DJ Jr, Rosenberg SA, Restifo NP. Adoptive immunotherapy for cancer: building on success. Nat Rev Immunol 2006;6:383-93.

31. Restifo NP, Dudley ME, Rosenberg SA. Adoptive immunotherapy for cancer: harnessing the T cell response. Nat Rev Immunol 2012;12: 269-81.

32. Ohigashi Y, Sho M, Yamada Y, Tsurui Y, Hamada K, Ikeda N, et al. Clinical significance of programmed death-1 ligand-1 and programmed death-1 ligand-2 expression in human esophageal cancer. Clin Cancer Res 2005;11:2947-53.

33. Gao J, Wu Y, Su Z, Barnie PA, Jiao Z, Qingli B, et al. Infiltration of alternatively activated macrophages in cancer tissue is associated with MDSC and Th2 polarization in patients with esophageal cancer. PLoS One 2014 Aug 21;9(8):e104453.

34. Muro K, Hamaguchi T, Ohtsu A, Boku N, Chin K, Hyodo I, et al. A phase II study of single-agent docetaxel in patients with metastatic esophageal cancer. Ann Oncol 2004;15:955-9.

35. Tew WP, Kelsen DP, Ilson DH. Targeted therapies for esophageal cancer. Oncologist 2005;10:590-601.

36. Shirakura Y, Mizuno Y, Wang L, Imai N, Amaike C, Sato E, et al. T-cell receptor gene therapy targeting melanoma-associated antigen-A4

inhibits human tumor growth in non-obese diabetic/SCID/γcnull mice. Cancer Sci 2012;103:17-25.

37. Muraoka D, Kato T, Wang L, Maeda Y, Noguchi T, Harada N, et al. Peptide vaccine induces enhanced tumor growth associated with apoptosis induction in CD8+ T Cells. J Immunol 2010;185:3768-76.
38. Hailemichael Y, Dai Z, Jaffarzad N, Ye Y, Medina MA, Huang XF, et al. Persistent antigen at vaccination sites induces tumor-specific $CD8^+$ T cell sequestration, dysfunction and deletion. Nat Med 2013;19:465-72.
39. Parkhurst MR, Yang JC, Langan RC, Dudley ME, Nathan DA, Feldman SA, et al. T cells targeting carcinoembryonic antigen can mediate regression of metastatic colorectal cancer but induce severe transient colitis. Mol Ther 2011;19:620-26.
40. Linette GP, Stadtmauer EA, Maus MV, Rapoport AP, Levine BL, Emery L, et al. Cardiovascular toxicity and titin cross-reactivity of affinity-enhanced T cells in myeloma and melanoma. Blood 2013;122:863-871.
41. Cameron BJ, Gerry AB, Dukes J, Harper JV, Kannan V, Bianchi FC, et al. Identification of a Titin-derived HLA-A1-presented peptide as a cross-reactive target for engineered MAGE A3-directed T cells. Sci Transl 2013;197ra103.

42. Morgan RA, Chinnasamy N, Abate-Daga D, Gros A, Robbins PF, Zheng Z, et al. Cancer regression and neurological toxicity following anti-MAGE-A3 TCR gene therapy. J Immunother 2013;36:133-51.

Figure Legends;

Figure 1.

Cell kinetics of MAGE-A4–specific TCR–transduced T cells after transfer into 10 patients. ***A.*** Panels show kinetics of 3 patients who received 2×10^8 cells, 4 patients who received 1×10^9 cells, and 3 patients who received 5×10^9 cells. Peripheral blood was collected at baseline and at pre-determined time points over a period of 63 days. DNA samples were extracted from the PBMCs, and TCR gene copy numbers were measured by quantitative PCR. The detection limit of the transduced cells is 100 copies/10^5 cells. ***B.*** Cell kinetics from day 1 to day 30. The kinetics are shown as logarithmic expressions. On days 14 and 28, MAGE-A4 peptides were given to all patients except TCR-MA-209. In Cohort 3, the peak levels ranged from 80–120 (x 10^3 copies/10^5 cells). The average number of the TCR-transgene per cell was 7 in the pre-infusion state, which indicates that 11–17% TCR-gene–transduced T cells appeared in the peripheral blood.

Figure 2.

Long-term cell kinetics of MAGE-A4–specific TCR–transduced T cells in 8 patients. Peripheral blood was collected on the day of patients' visits to the clinic after 35 days. DNA samples were extracted from the PBMCs, and TCR gene copy numbers were measured by quantitative PCR. The detection limit

of the transduced cells is 100 copies/10^5 cells. MAGE-A4 peptides were also vaccinated on the same day, as indicated in the case of TCR-MA-208.

Figure 3.

Tetramer analysis of the TCR-gene–transduced T cells at pre-infusion and peripheral T cells after adoptive transfer of TCR-transduced T cells.
A. PBMCs were collected 3 days after the adoptive transfer of TCR-transduced lymphocytes, and directly stained with MAGE-A4 peptide/HLA-A*24:02 tetramer in 9 patients. ***B.*** PBMCs collected from TCR-MA-102, before and after transfer of TCR-transduced lymphocytes. CD8+ T cells were selected, stimulated in vitro with MAGE-A4 peptide, and assayed for tetramer of MAGE-A4 peptide/HLA-A*24:02. Irrelevant peptide/HLA-A*24:02 tetramers were used as a control. ***C.*** T-cell clones were established from PBMCs of TCR-MA-102 on days 28 and 105. The cloned cells were derived from the MAGE-A4 peptide/HLA-A*24:02 tetramer+ and tetramer- fractions. ***D.*** PBMCs collected from TCR-MA-106, -208 and -212 before and after transfer of TCR-transduced lymphocytes. CD8+ T cells were selected, stimulated in vitro with MAGE-A4 peptide, and assayed for MAGE-A4 peptide/HLA-A*24;02 tetramers.

Figure 4.

Reactivity to MAGE-A4 peptide and MAGE-A4+ tumor cells in PBMCs after TCR-transduced T cell transfer. PBMCs collected from TCR-MA-106, -208, and -212, before and after transfer of TCR-transduced lymphocytes. CD8+ T cells were selected, stimulated in vitro with MAGE-A4 peptide, and subjected to ELISPOT assays. The target cells were 11-18 (MAGE-A4+, HLA-A*24:02+), QG-56 (MAGE-A4+, HLA-A*24:02-) and T2A24 cells pulsed with MAGE-A4 peptide. T2A24 cells pulsed with an irrelevant peptide were used as control targets.

Figure. 1

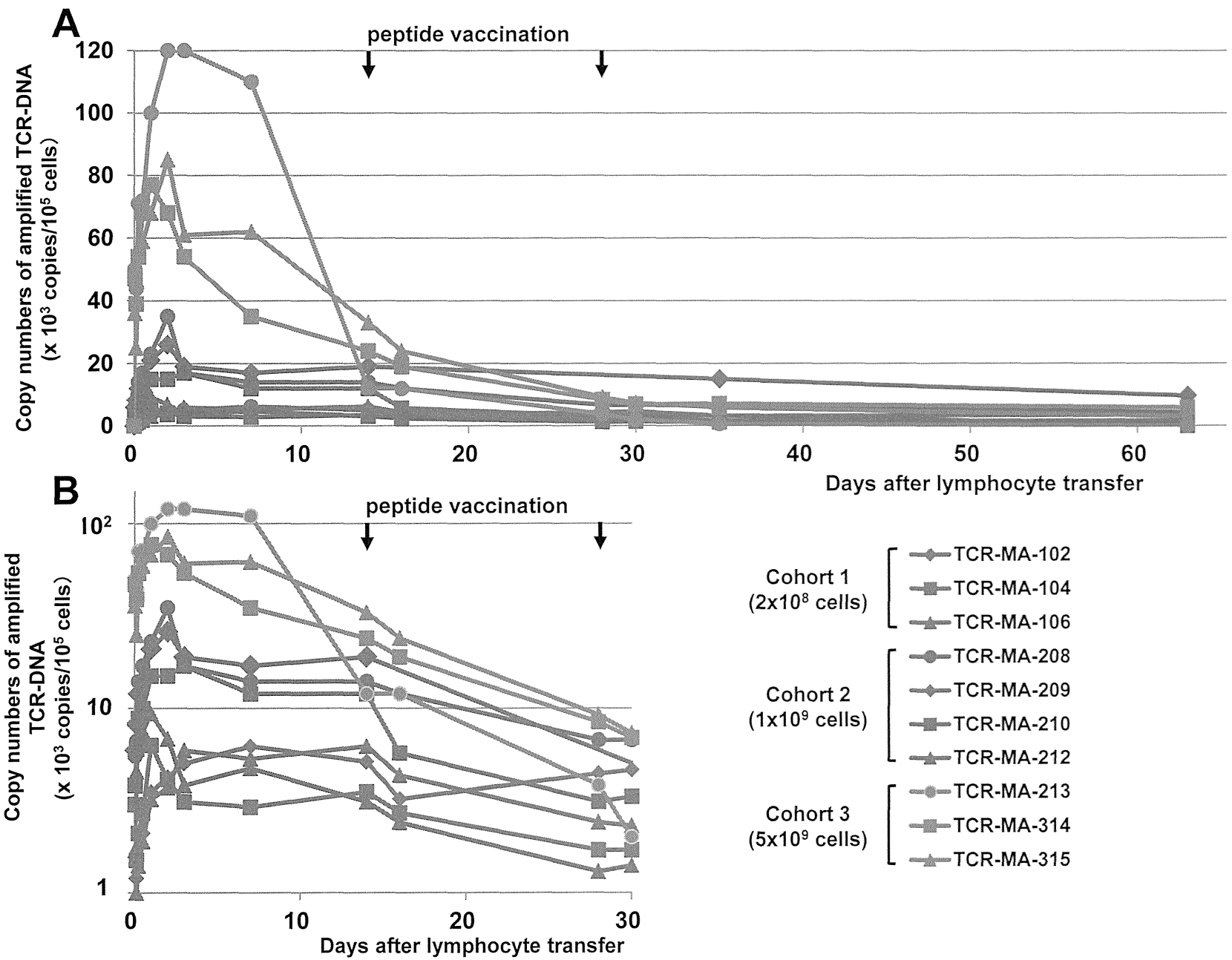
A
peptide vaccination
Copy numbers of amplified TCR-DNA (x 10³ copies/10⁵ cells)
120
100
80
60
40
20
0
0
10
20
30
40
50
60
Days after lymphocyte transfer
B
peptide vaccination
Copy numbers of amplified TCR-DNA (x 10³ copies/10⁵ cells)
10²
10
1
0
10
20
30
Days after lymphocyte transfer
Cohort 1 (2x10⁸ cells)
TCR-MA-102
TCR-MA-104
TCR-MA-106
Cohort 2 (1x10⁹ cells)
TCR-MA-208
TCR-MA-209
TCR-MA-210
TCR-MA-212
Cohort 3 (5x10⁹ cells)
TCR-MA-213
TCR-MA-314
TCR-MA-315

Figure. 2

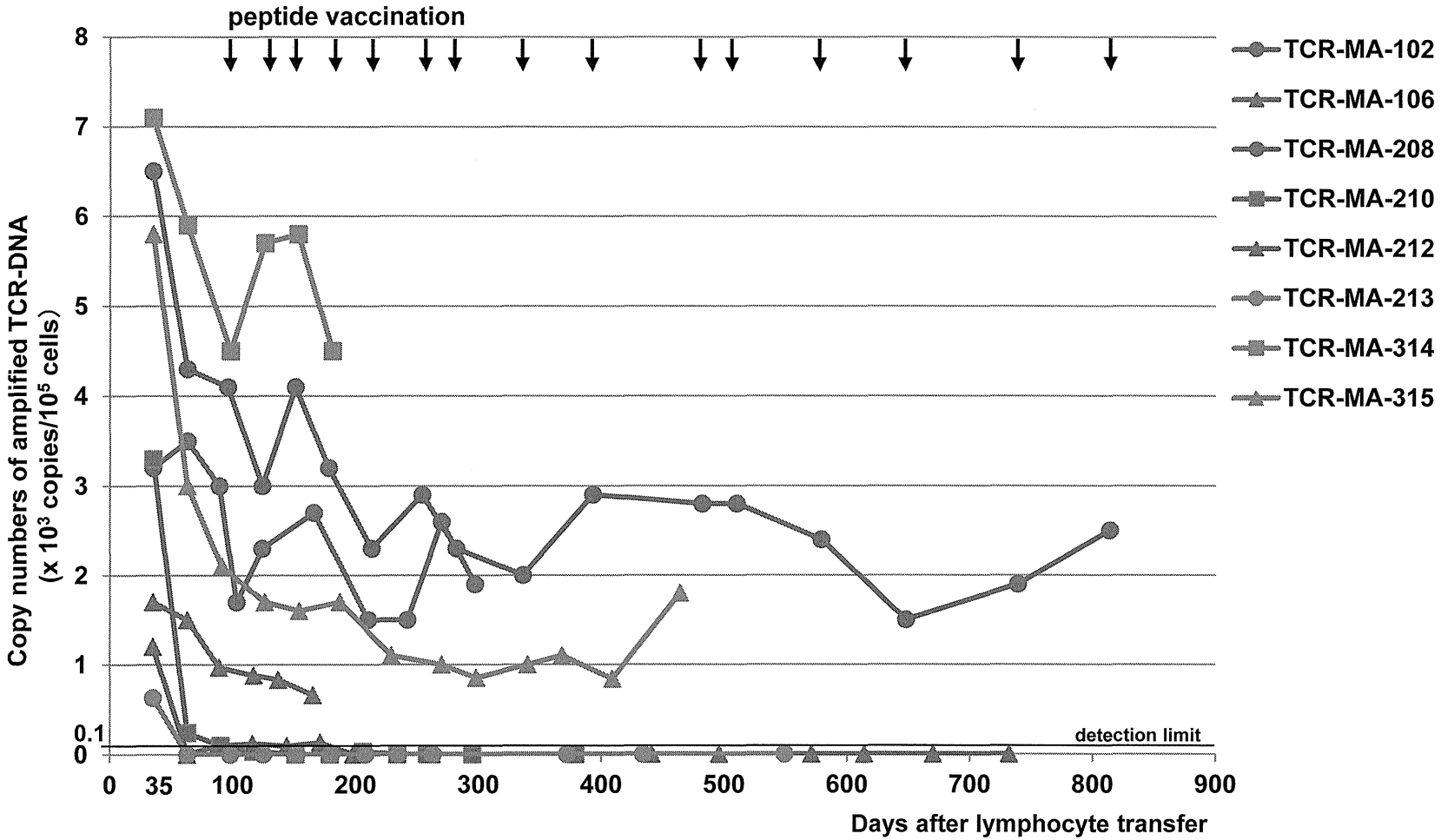
peptide vaccination
Copy numbers of amplified TCR-DNA
(x 10³ copies/10⁵ cells)
8
7
6
5
4
3
2
1
0.1
0
detection limit
0
35
100
200
300
400
500
600
700
800
900
Days after lymphocyte transfer
TCR-MA-102
TCR-MA-106
TCR-MA-208
TCR-MA-210
TCR-MA-212
TCR-MA-213
TCR-MA-314
TCR-MA-315

Figure. 3

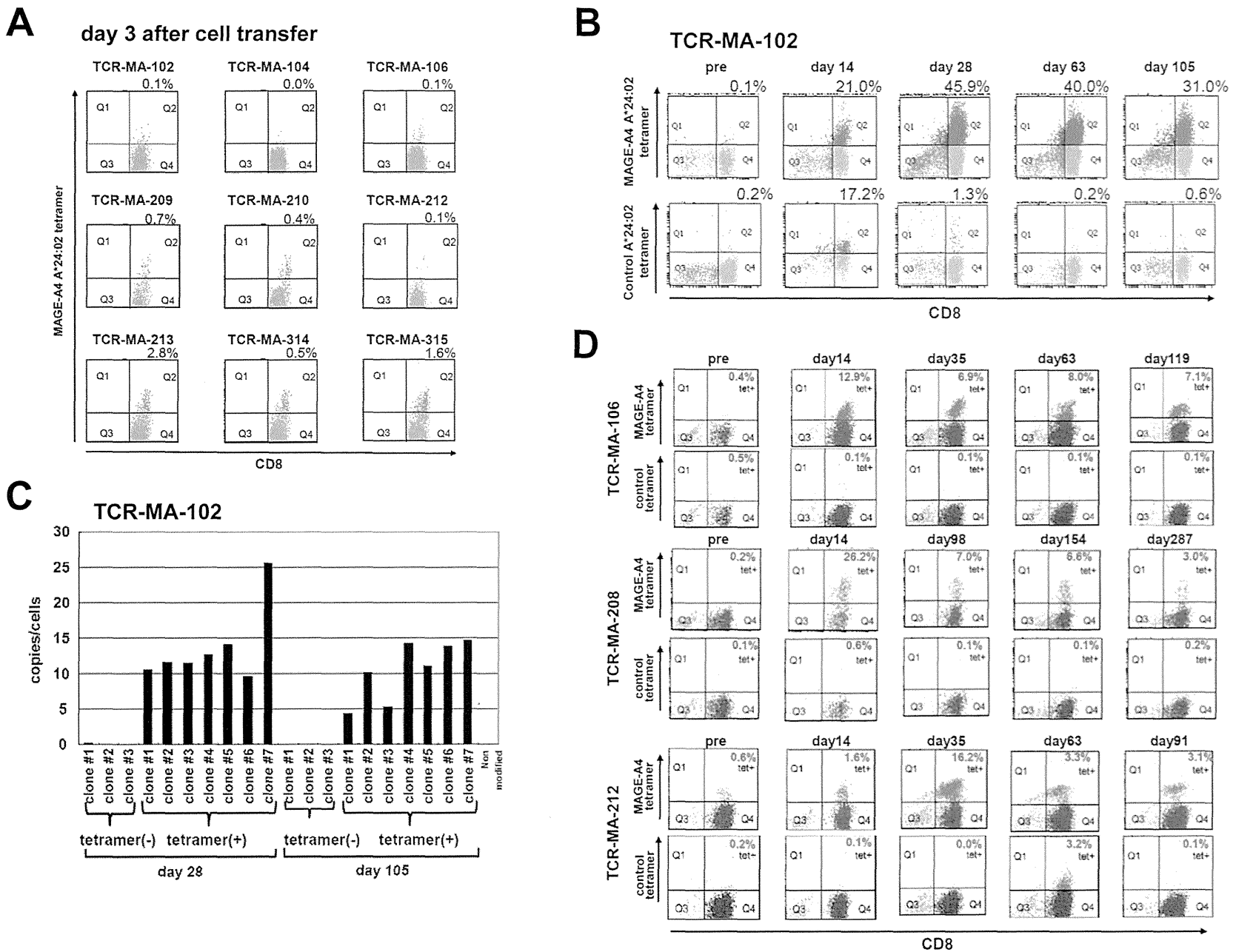
A
day 3 after cell transfer
TCR-MA-102
0.1%
TCR-MA-104
0.0%
TCR-MA-106
0.1%
TCR-MA-209
0.7%
TCR-MA-210
0.4%
TCR-MA-212
0.1%
TCR-MA-213
2.8%
TCR-MA-314
0.5%
TCR-MA-315
1.6%
MAGE-A4 A*24:02 tetramer
CD8
B
TCR-MA-102
pre
day 14
day 28
day 63
day 105
MAGE-A4 A*24:02 tetramer
0.1%
21.0%
45.9%
40.0%
31.0%
Control A*24:02 tetramer
0.2%
17.2%
1.3%
0.2%
0.6%
CD8
C
TCR-MA-102
copies/cells
clone #1
clone #2
clone #3
clone #4
clone #5
clone #6
clone #7
Non modified
tetramer(-)
tetramer(+)
day 28
day 105
D
TCR-MA-106
TCR-MA-208
TCR-MA-212
MAGE-A4 tetramer
control tetramer
pre
day14
day35
day63
day119
day98
day154
day287
day91
tet+
CD8

Figure. 4

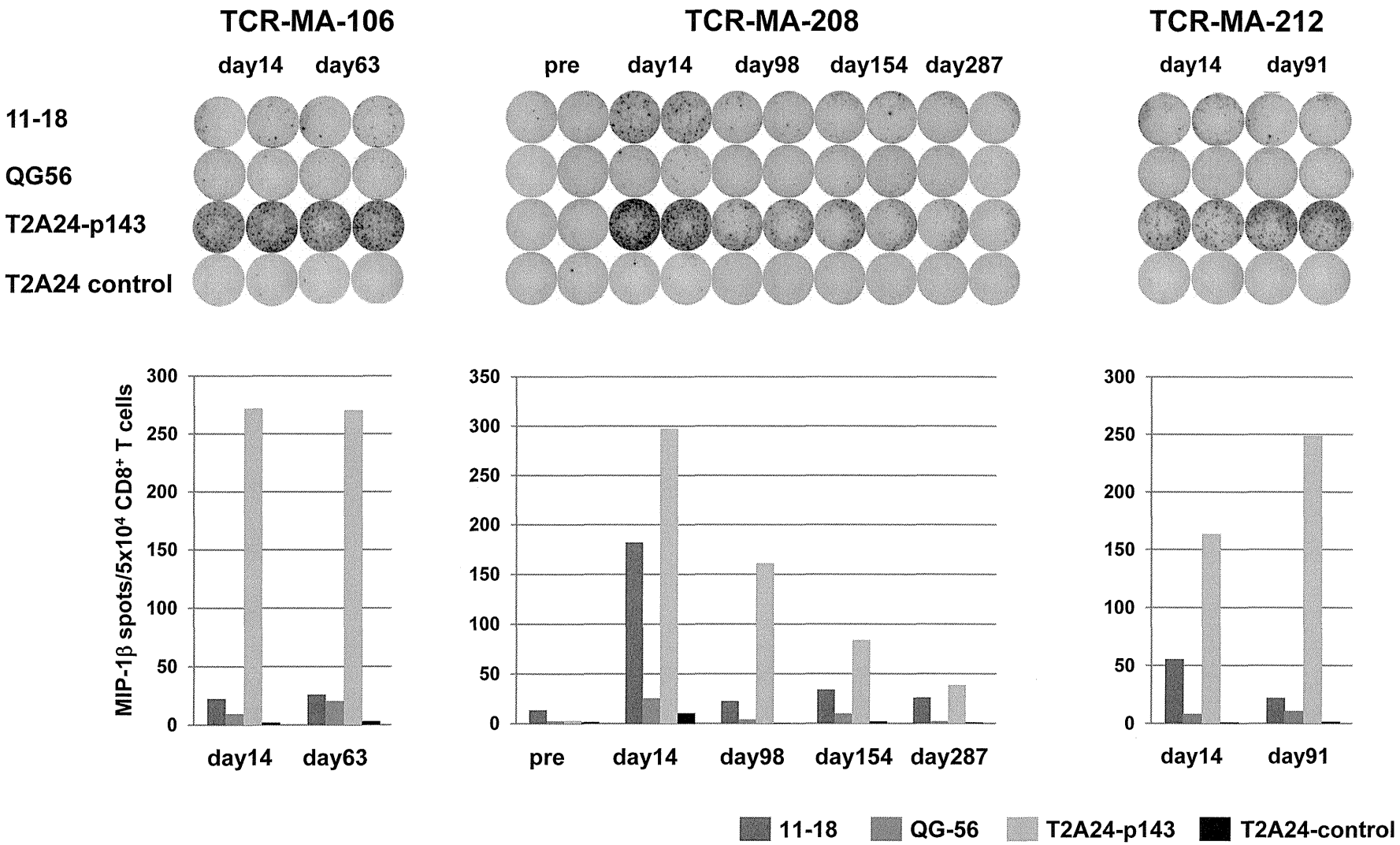
TCR-MA-106
day14
day63
TCR-MA-208
pre
day14
day98
day154
day287
TCR-MA-212
day14
day91
11-18
QG56
T2A24-p143
T2A24 control
MIP-1β spots/5x10⁴ CD8⁺ T cells
300
250
200
150
100
50
0
350
300
250
200
150
100
50
0
day14
day63
pre
day14
day98
day154
day287
day14
day91
11-18
QG-56
T2A24-p143
T2A24-control

Table 1. Phenotypes of manufactured lymphocytes after TCR-gene transduction

Patient ID	CD3 (%)	CD4 (%)	CD8 (%)	MAGE-A4 tetramer+ cells		IFN-γ responded cells*		Copies of TCR-transgene/cell
				CD8- cells(%)	CD8+ cells(%)	CD8- cells(%)	CD8+ cells(%)	
TCR-MA-102	89.4	59.9	30.3	4.5	6.3	6.6	24.3	5.4
TCR-MA-104	91.8	71.7	27.1	0.5	1.8	5.5	23.1	5.1
TCR-MA-106	96.7	29.3	76.8	0.3	8.6	3.6	9.7	6.9
TCR-MA-208	95.5	81.1	17.6	8.5	4.1	22.4	38.9	10.0
TCR-MA-209	97.9	57.5	45.4	2.6	7.9	21.8	28.8	8.8
TCR-MA-210	94.7	40.9	60.5	3.3	11.1	7.3	15.9	8.3
TCR-MA-212	99.7	14.1	88.9	0.6	12.6	7.5	29.6	10.1
TCR-MA-213	95.6	47.2	54.1	2.8	9.1	9.1	19.6	9.9
TCR-MA-314	97.6	41.1	59.9	1.0	1.5	4.9	22.1	7.1
TCR-MA-315	89.8	54.1	45.3	2.6	4.5	18.2	43.1	8.7

* IFN-γ releasing cells responded by peptide-pulsed target cells.

Table 2. Patients characteristics and adverse events after TCR-gene transduced lymphocytes transfer

Cohort	Cell doses allocated	Patient ID	Age/sex	MAGE-A4 expressions				Previous therapy			Tumor lesions	Number of IFN-γ+ CD8+ T cell infused	Adverse events (grade)
				PCR*	IHC†/57B Ab	IHC**/MCV-1 Ab	IHC**/MCV-4 Ab	surgery	radiotherapy	chemotherapy			
1	$2x10^8$	TCR-MA-102	68/M	2,880		NA		-	+	CDDP/5-FU	liver	1.46x10^7	none
	$2x10^8$	TCR-MA-104	56/M	4,847	20%	20%	20%	-	+	CDDP/5-FU	esophagus	1.24x10^7	none
	$2x10^8$	TCR-MA-106	73/M	2,215	10%	0	5%	-	+	CDDP/5-FU, TS-1	esophagus, lymph node	1.48x10^7	skin reaction(I)§
2	$1x10^9$	TCR-MA-208	67/M	7,942	30%	90%	10%	-	+	CDDP/5-FU	lymph node‡	6.8x10^7	none
	$1x10^9$	TCR-MA-209	57/M	1,352	70%	10%	50%	+	+	CDDP/5-FU	lymph node	1.3x10^8	none
	$1x10^9$	TCR-MA-210	54/M	312	30%	20%	20%	-	-	CDDP/5-FU, Docetaxel	esophagus, lung, lymph node	9.6x10^7	skin reaction(I)§
	$1x10^9$	TCR-MA-212	43/M	1,765	20%	10%	5%	+	+	CDDP/5-FU, docetaxel	lymph node‡	2.6x10^8	skin reaction(I)§
3	$5x10^9$	TCR-MA-213	68/M	749		NA		+	+	CDDP/5-FU	lymph node‡	5.3x10^8	none
	$5x10^9$	TCR-MA-314	64/M	82	focal	focal	focal	+	+	CDDP/5-FU	lymph node	6.6x10^8	none
	$5x10^9$	TCR-MA-315	57/F	NA	20%	20%	20%	+	+	CDDP/5-FU	lung, lymph node	9.75x10^8	skin reaction(I)§

* Copies numbers amlified by RealTime PCR. † Positive percentage in tumor samples by immunohistochemical staining.

‡ Minimal lesions, unable to evaluate by RECIST. § Skin reactions were related to peptide vaccinations.

Abbreviations; NA, not available; IHC, immunohistochemistry.

Brief Report

IMMUNOBIOLOGY

Histone deacetylase inhibition regulates inflammation and enhances Tregs after allogeneic hematopoietic cell transplantation in humans

Sung Won Choi,[1] Erin Gatza,[1] Guoqing Hou,[1] Yaping Sun,[2] Joel Whitfield,[3] Yeohan Song,[1] Katherine Oravecz-Wilson,[2] Isao Tawara,[4] Charles A. Dinarello,[5] and Pavan Reddy[2]

[1]Department of Pediatrics, [2]Department of Internal Medicine, Division of Hematology-Oncology, Blood and Marrow Transplantation Program, and [3]Immunology Core, Comprehensive Cancer Center, University of Michigan, Ann Arbor, MI; [4]Department of Hematology-Oncology, Mie University Hospital, Tsu, Mie, Japan; and [5]Department of Medicine, Division of Infectious Diseases, University of Colorado, Aurora, CO

Key Points

- HDAC inhibition reduced proinflammatory cytokines and increased regulatory T-cell number and function after allo-HCT.
- HDAC inhibition enhanced signal transducer and activator of transcription 3 acetylation and induced indoleamine-2,3-dioxygenase after allo-HCT.

We examined immunological responses in patients receiving histone deacetylase (HDAC) inhibition (vorinostat) for graft-versus-host disease prophylaxis after allogeneic hematopoietic cell transplant. Vorinostat treatment increased histone acetylation in peripheral blood mononuclear cells (PBMCs) from treated patients, confirming target HDAC inhibition. HDAC inhibition reduced proinflammatory cytokine levels in plasma and from PBMCs and decreased ex vivo responses of PBMCs to proinflammatory TLR-4 stimuli, but did not alter the number or response of conventional T cells to nonspecific stimuli. However, the numbers of regulatory T cells (Tregs) were increased, which revealed greater demethylation of the Foxp3 T regulatory-specific demethylation region. Vorinostat-treated patients showed increased expression of CD45RA and CD31 on Tregs, and these Tregs demonstrated greater suppression on a per cell basis. Consistent with preclinical findings, HDAC inhibition also increased signal transducer and activator of transcription 3 acetylation and induced indoleamine-2,3-dioxygenase. Our data demonstrate that HDAC inhibition reduces inflammatory responses of PBMC but enhances Tregs after allo-HCT. (*Blood.* 2015;125(5):815-819)

Introduction

Acute graft-versus-host disease (GVHD) remains a major contributor of nonrelapse mortality after allogeneic hematopoietic cell transplant (allo-HCT).[1] Its pathogenesis involves a complex network of interactions among alloreactive T cells, antigen-presenting cells (APCs), proinflammatory cytokines, and effector cells, leading to target organ injury in the host.[2] In experimental models of allo-HCT, a histone deacetylase (HDAC) inhibitor (vorinostat) reduced proinflammatory cytokines[3] through the induction of indoleamine-2,3-dioxygenase (IDO) in a signal transducer and activator of transcription 3 (STAT-3)-dependent manner[4,5] and increased regulatory T cells (Tregs)[6] to attenuate GVHD. On the basis of these experimental observations, we recently performed a clinical trial of HDAC inhibition after allo-HCT that demonstrated significantly decreased acute GVHD without an increase in relapse.[7] However, whether HDAC inhibition had a similar immunologic effect on inflammatory cell and Treg responses in humans is not known.[8] In the present study, we explored the role of HDAC inhibition on inflammation, conventional T cells (Tconvs), and Tregs in patients from the clinical trial[7] of vorinostat after allogeneic transplant.

Study design

Study cohort and sample collection

Laboratory studies were conducted in 50 patients who underwent a clinical trial.[7] Oral vorinostat was administered 10 days before the stem cell infusion and continued until day 100. Study patients were compared with patients who were similarly transplanted and given standard-of-care treatment but did not receive vorinostat (control cohort). Samples were collected under informed consents and institutional review board-approved research protocols.[7] Research was conducted in accordance with the Declaration of Helsinki. No differences in clinical characteristics were observed between study participants and the control cohort (supplemental Table 1, available on the *Blood* Web site).

Immunoblotting

Histones and STAT-3 in peripheral blood mononuclear cells (PBMCs) were assessed by western blot, as previously described,[7] using antibodies listed in the supplemental Methods.

Cytokine analyses

Cytokine production was determined in plasma and PBMC supernatant samples by ELISA and in $CD11c^+$ PBMCs by intracellular staining, as previously described.[7]

Submitted October 7, 2014; accepted November 20, 2014. Prepublished online as *Blood* First Edition paper, November 26, 2014; DOI 10.1182/blood-2014-10-605238.

The online version of this article contains a data supplement.

The publication costs of this article were defrayed in part by page charge payment. Therefore, and solely to indicate this fact, this article is hereby marked "advertisement" in accordance with 18 USC section 1734.

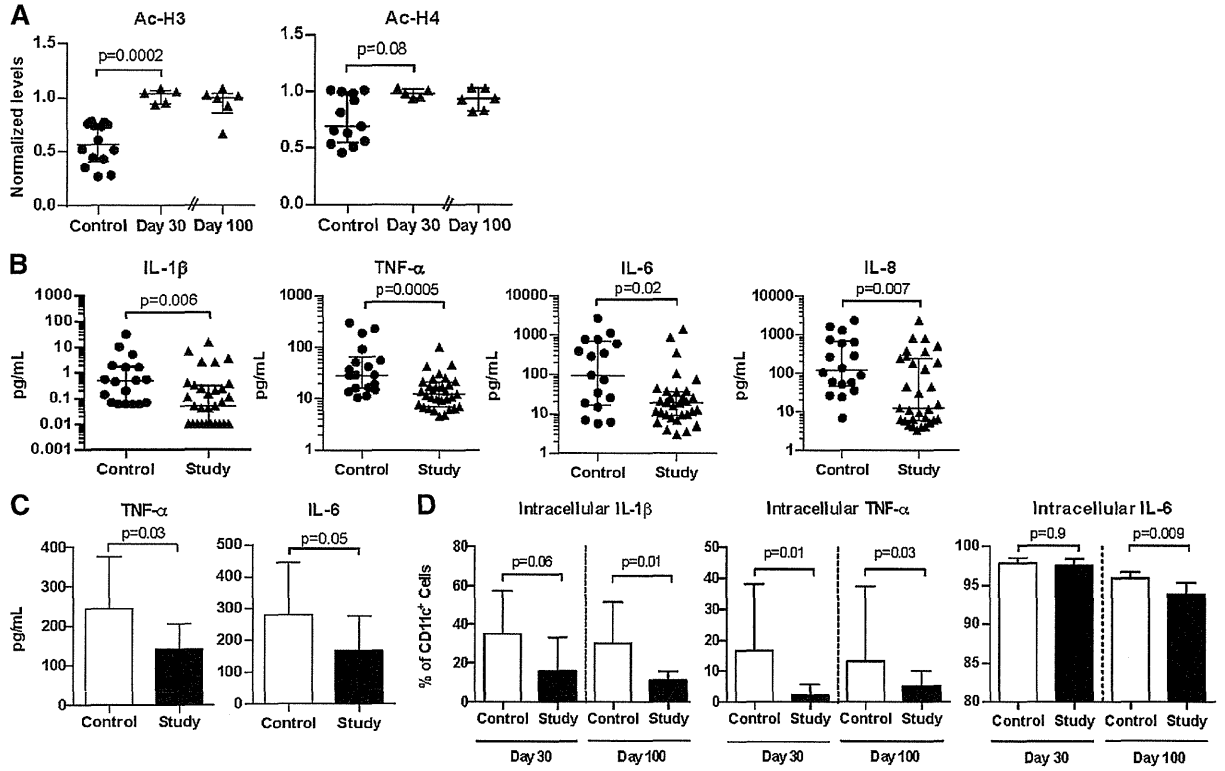

Figure 1. HDAC inhibition modulated histone acetylation and proinflammatory cytokine production after human allo-HCT. Triangles and black bars denote patients in the study who received vorinostat. Circles and open bars denote control patients who did not receive vorinostat. Median values ± interquartile range are plotted. Each data point in a dot plot represents a single patient. All plots include data from at least 2 independent experiments. (A) Levels of acetylated (Ac-) H3 and H4 30 and 100 days after allo-HCT. Levels in each patient normalized to β-actin. (B) Levels of interleukin 1β (IL-1β), tumor necrosis factor α (TNF-α), IL-6, and IL-8 in the plasma of study patients and control patients 14 days after allo-HCT. Control, n = 18; study, n = 31. (C) TNF-α and IL-6 production by PBMC after ex vivo stimulation with lipopolysaccharide (500 ng/mL) for 16 to 24 hours, 30 days after allo-HCT. Control, n = 12; study, n = 14. (D) Intracellular staining of IL1-β, TNF-α, and IL-6 in $CD11c^+$ PBMCs of study and control patients 30 and 100 days after allo-HCT, after ex vivo stimulation with phorbol 12-myristate 13-acetate (PMA) and ionomycin. Day 30: control, n = 6; study, n = 10. Day 100: control, n = 6; study n = 6.

Phenotype of T lymphocytes

Routine absolute lymphocyte counts were performed in the Clinical Hematology Laboratory. To enumerate $CD4^+$, $CD8^+$, and Treg cells, PBMCs were stained using fluorochrome-conjugated antihuman monoclonal antibodies detailed in the supplemental Methods. To detect recent thymic emigrants (RTEs), PBMCs were identified using anti-human CD4, CD25, CD31, and CD45RA.[9]

RNA isolation and real-time-polymerase chain reaction

Total cellular RNA was isolated from PBMCs, reverse-transcribed, and used for real-time polymerase chain reaction analysis of Foxp3 and IDO, using previously described methods and primer pairs.[7]

Treg-specific-demethylation region demethylation assay

$CD4^+CD25^+$ Tregs and $CD4^+CD25^-$ Tconvs were sorted from PBMCs using the Regulatory T Cell Kit (Miltenyi Bioscience, Bergisch Gladbach, Germany). Genomic DNA was isolated and Treg-specific-demethylation region (TSDR) analysis performed as previously described.[9,10] Polymerase chain reaction conditions and specific primers pairs are listed in the supplemental Methods.

Treg suppression assay

Tregs and Tconvs were isolated, as described earlier. Tregs were mixed at ratios of 1:4 and 1:8 with Tconvs and incubated with the presence of anti-CD3/anti-CD28 coated beads (Life Technologies, Grand Island, NY) for 72 hours. ^{3}H-thymidine (1 μCi/well; NEN Life Sciences Products, Zaventem, Belgium) was incorporated by proliferating cells for the last 8 hours of incubation and was measured using a TopCount NXT Microplate Scintillation Counter (Perkin Elmer, Waltham, MA).

Statistical analysis

Samples from the study and control cohorts were compared using the Mann-Whitney nonparametric test. Comparison of paired samples from the same patient was made using the Wilcoxon matched-pairs signed rank nonparametric test. These statistical analyses were performed using GraphPad Prism 6.0 (GraphPad Software, Inc, La Jolla, CA). A 2-sided *P*-value of less than .05 indicated statistical significance.

Results and discussion

Administration of vorinostat increased H3 and H4 acetylation, confirming HDAC inhibition,[8,11] and these increases had prolonged effects without significant decline 100 days after transplant (Figure 1A; supplemental Figure 1). Because HDAC inhibition mitigated inflammation and reduced GVHD in preclinical models,[1-4,8] we explored the effect of vorinostat on inflammatory cell responses. Similar to preclinical observations, vorinostat-treated patients experienced significant reductions in the plasma levels of proinflammatory cytokines such as IL-1β, TNF-α, IL-6, and IL-8 14 days after

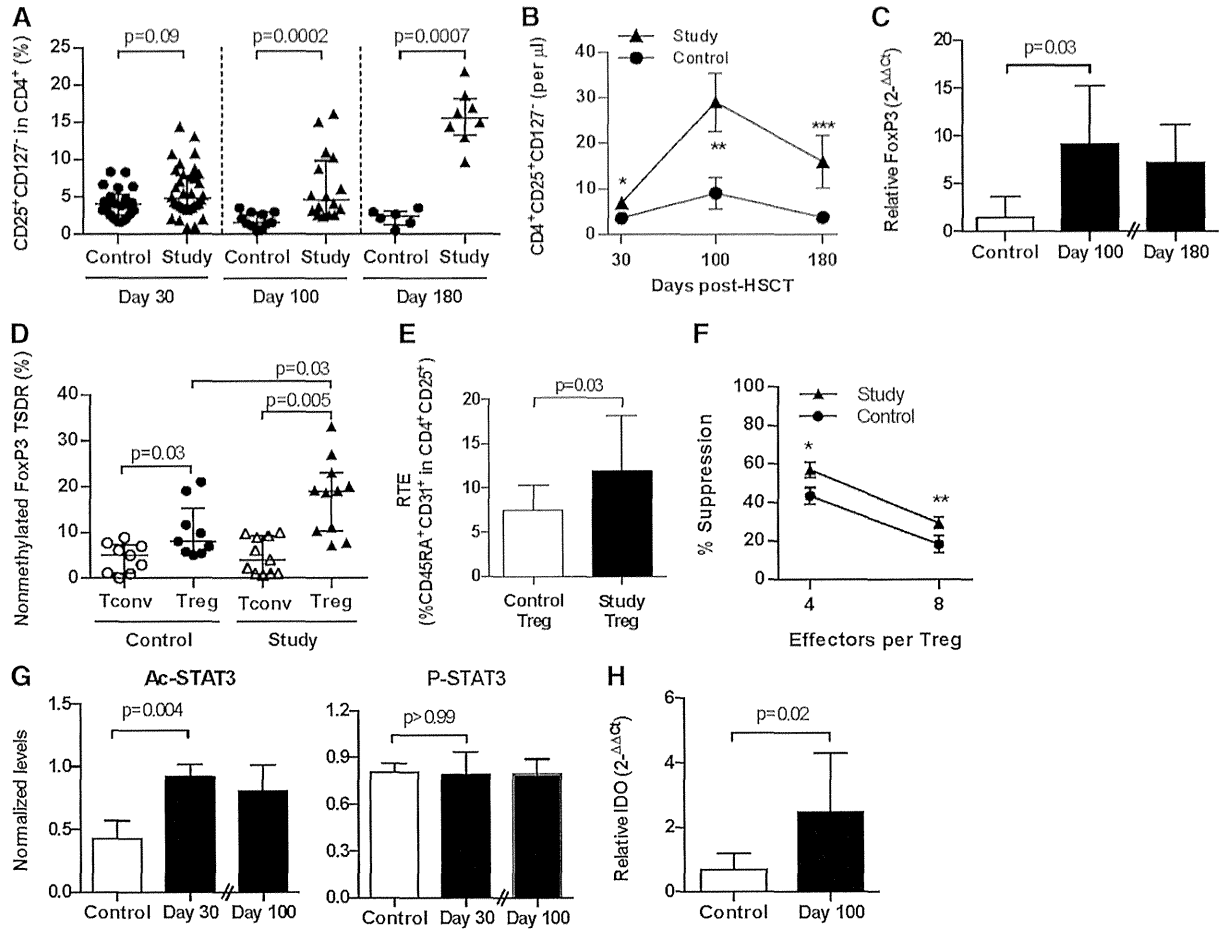

Figure 2. Patients treated with vorinostat have increased Tregs with greater suppressive function and increased acetylation of STAT-3 and IDO expression after allo-HCT. Triangles and black bars denote patients who received vorinostat. Circles and open bars denote control patients. All plots include, or are representative of, data from at least 2 independent experiments. Mean values ± SEM are plotted in B and F. Median values ± interquartile range are plotted in all other panels. (A-B) $CD25^+CD127^-$ cells within the $CD4^+$ population of PBMCs 30, 100, and 180 days after allo-HCT. Day 30: control, n = 22; study, n = 36. Day 100: control, n = 11; study, n = 16. Day 180: control, n = 6; study, n = 8. *Control vs study, $P = .01$; **$P = .007$; ***$P = .06$. (C) Foxp3 expression in PBMCs 100 and 180 days after allo-HCT. Data are expressed relative to glyceraldehyde-3-phosphate dehydrogenase copy number. Day 100: control, n = 6; study, n = 6. Day 180: study, n = 9. (D) Methylation of the Foxp3 TSDR in purified $CD4^+CD25^-$ conventional (Tconv, open icons) and $CD4^+CD25^+$ regulatory (Treg, black icons) T cells 100 days after allo-HCT. Control, n = 9; study, n = 11. (E) $CD4^+CD25^+CD45RA^+CD31^+$ RTE 100 days after allo-HCT. Control, n = 5; study, n = 6. (F) Suppression of effector Tconv proliferation to anti-CD3 and anti-CD28 stimulation by autologous Tregs 100 days after allo-HCT. Control, n = 8; study, n = 10. *$P = .04$; **$P = .07$. (G) Levels of Ac- and phosphorylated (P)-STAT-3 30 and 100 days after allo-HCT. Ac- and P-STAT-3 levels normalized to total STAT-3. Day 30, control, n = 3 to 6; study, n = 5; Day 100: study, n = 6. (H) IDO messenger RNA (mRNA) expression 100 days after allo-HCT. Values are expressed relative to glyceraldehyde-3-phosphate dehydrogenase mRNA copy number. Control, n = 6; study, n = 6.

transplant (Figure 1B). Interferon γ, IL-17, and IL-2 cytokines were also evaluated at this point. Although IL-17 was significantly reduced, interferon γ and IL-17 were not different between the study and control cohorts (supplemental Figure 2). We measured plasma cytokines 30 days after transplant and found significant reductions in TNF receptor-1 and IL-8 levels (supplemental Figure 3). Although plasma IL-6 levels were reduced in vorinostat-treated patients, statistical significance was not reached. IL-1β was also unchanged at day 30 between the 2 cohorts (supplemental Figure 3). Furthermore, we measured plasma biomarkers of GVHD 14 and 30 days posttransplant,[12,13] such as regenerating islet-derived 3-α, suppressor of tumorigenicity 2, IL-2Rα, hepatocyte growth factor, and Elafin (supplemental Table 2). We did not find a clear correlation with clinical outcomes, which we speculate may have been a result of the conditioning regimen (reduced intensity) and the small number of patients who developed GVHD in our study.[7]

HDAC inhibition also reduced the release of proinflammatory cytokines by PBMCs ex vivo in response to lipopolysaccharide (Figure 1C) and by $CD11c^+$ after PMA/ionomycin stimulation of bulk PBMCs (Figure 1D). These observations of reduced proinflammatory cytokines in the presence of HDAC inhibition are also consistent with other studies.[14,15] Importantly, we did not observe significant differences in percentages of $CD19^+$, $CD14^+$, or $CD11c^+$ cells in the PBMCs of study patients compared with controls (supplemental Table 3), nor did the percentage of $CD11c^+$ PBMC differ between groups after PMA/ionomycin stimulation (data not shown). In contrast to preclinical findings,[3] expression of MHC class II or costimulatory (CD86) molecules by $CD11c^+$ PBMC were not changed in patients treated with vorinostat on either day 30 (supplemental Table 3) or 100 days posttransplant (data not shown).

Patients with GVHD have reduced frequencies of Tregs.[16-18] In murine models, Tregs attenuate GVHD,[19] and HDAC inhibition

increased Treg numbers and enhanced their suppressive function but did not directly alter non-Treg, that is, Tconv, responses.[3,6,14,20] HDAC inhibition can also enhance suppression by human Tregs[21] and promote the conversion of human T cells into Tregs in vitro.[22] We therefore explored the effect of HDAC inhibition with vorinostat on both Tregs and Tconv after clinical allogeneic BMT. HDAC inhibition did not significantly alter total lymphocyte or $CD4^+$ or $CD8^+$ T-cell counts, nor did it alter the proliferative response of Tconv to nonspecific stimuli (supplemental Table 4; supplemental Figure 4). However, patients treated with vorinostat exhibited increased numbers of Tregs ($CD4^+CD25^+CD127^-$) in the peripheral circulation (Figure 2A-B; supplemental Figure 5). Consistent with this increase, Foxp3 mRNA expression was increased in PBMC 30 days after transplant,[7] which remained significantly higher 100 days posttransplant (Figure 2C). Foxp3 expression was verified on a per cell basis by flow cytometry, where more than 80% of $CD4^+CD25^+CD127^-$ cells were $Foxp3^+$ (data not shown).

Foxp3 is a critical regulator of Treg development and function[23] and is subject to epigenetic regulation through methylation of cytosine guanine dinucleotide islands within the TSDR.[24] Thymus-derived Tregs with stable expression of Foxp3 show TSDR demethylation, whereas recently activated conventional human T cells and Tregs induced in the periphery with transient Foxp3 expression show methylated TSDR.[25] HDAC inhibition with vorinostat increased demethylation of the Foxp3 TSDR in $CD4^+CD25^+$ T cells 100 days posttransplant (Figure 2D). Consistent with increased TSDR demethylation, HDAC inhibition also increased the numbers of $CD45RA^+CD31^+$ Treg RTEs (Figure 2E; supplemental Figure 6), whereas Tconv RTEs ($CD4^+CD25^-CD45RA^+CD31^+$) were not changed ($P = .42$; data not shown). Preliminary analysis also demonstrated a trend toward increased TRECs in $CD4^+CD25^+$ Treg (supplemental Figure 7). Thus, although we cannot rule out the possibility that vorinostat also induced Tregs in the periphery, the data suggest that at least a portion of the increased Tregs observed in study patients were natural Tregs derived from the thymus. We next determined the functionality of these Tregs. Tregs isolated from vorinostat-treated patients suppressed effector T-cell proliferation more effectively on a per cell basis (Figure 2F). However, antigen-specific functional studies (eg, recovery of CMV- or EBV-specific T cells) were not performed.

HDAC inhibition in mice increased acetylation of the nonhistone protein STAT-3,[5] which is critical for the induction of IDO in APCs,[4] reduction in inflammation, and the regulation of acute GVHD.[4] Because vorinostat reduced acute GVHD[7] and mitigated inflammatory cytokines, we next analyzed STAT-3 acetylation and IDO induction in these patients. Concordantly, levels of Ac-STAT-3 protein were significantly increased with HDAC inhibition 30 days posttransplant, and levels remained high at day 100 (Figure 2G). P-STAT-3 levels were unchanged (Figure 2G), consistent with a previous study.[26] IDO is an intracellular enzyme that degrades tryptophan, suppresses APC function, and induces T-cell anergy.[27] IDO mRNA was also induced with HDAC inhibition on day 30 posttransplant ($P < .0001$)[7] and remained high at day 100 (Figure 2H).

Our data in murine models of HCT have shown that vorinostat modulates the production of inflammatory cytokines and induces IDO expression by host APCs to modulate GVHD after allo-HCT.[3-5] Additional murine data by others indicate that HDAC inhibitors promote the generation and function of regulatory T cells.[6] Ex vivo studies using human cells have confirmed the abilities of HDAC inhibitors to modulate both APCs and Tregs.[20,22] Thus, collective findings suggest that HDAC inhibition can have potent and distinct direct regulatory effects on various immune cell populations. Although the mouse continues to be an important in vivo model for human immunology, we understand that potential limitations of extrapolating data from mice to humans exist.[28] It is likely significant that human recipients of allo-HCT receive treatment with vorinostat concomitant with immunosuppressive therapy (tacrolimus and mycophenolate mofetil). It is possible that our inability to find quantitative reproducible differences in HLA and costimulatory molecule expression in human PBMC samples is reflective of direct effects of immunosuppression on APCs. Additional ex vivo analysis will be required to investigate this possibility. Nonetheless, the findings here demonstrate that HDAC inhibition with vorinostat after allo-HCT in humans regulated inflammation and enhanced Tregs. They further suggest that regulation of inflammation and increased Tregs might have been crucial for the ability to reduce clinical GVHD in the first-in-human clinical trial,[7] and collectively, suggest that HDAC inhibition has immune-regulatory effects in humans. Future studies are needed to further delineate which immune cells are affected by HDAC inhibition after allo-HCT.

Acknowledgments

This work was supported by the Leukemia and Lymphoma Society, the National Institutes of Health (National Cancer Institute grant R01CA143379 [P.R.], and National Institute of Allergy and Infectious Diseases grants 1K23AI091623 [S.W.C.], and AI-15614 [C.A.D.]), the A. Alfred Taubman Institute Emerging Scholar Program, and the Michigan Institute for Clinical and Health Research (UL1TR00043).

Authorship

Contribution: S.W.C. and P.R. designed the clinical trial and the laboratory experiments, reviewed clinical and laboratory data, and wrote the manuscript; E.G. reviewed laboratory data, designed and analyzed laboratory experiments, and wrote the manuscript; G.H. performed and analyzed laboratory experiments and reviewed and helped write the manuscript; Y. Sun designed and performed experiments related to immunoblotting and PCRs; Y. Song reviewed laboratory data and prepared figures for publication and reviewed the manuscript; I.T. performed and analyzed laboratory experiments; C.A.D. analyzed data and reviewed and helped write the manuscript; K.O.-W. and J.W. contributed to the experiments and reviewed and helped write the manuscript; and all authors vouch for the accuracy and completeness of the data and for the analyses.

Conflict-of-interest disclosure: The authors declare no competing financial interests.

Correspondence: Pavan Reddy, Blood and Marrow Transplantation Program, University of Michigan, 1500 E Medical Center Dr, 3312 Cancer Center, Ann Arbor, MI, 48109-5942; e-mail: reddypr@umich.edu.

References

1. Choi SW, Reddy P. Current and emerging strategies for the prevention of graft-versus-host disease. *Nat Rev Clin Oncol.* 2014;11(9):536-547.
2. Blazar BR, Murphy WJ, Abedi M. Advances in graft-versus-host disease biology and therapy. *Nat Rev Immunol.* 2012;12(6):443-458.
3. Reddy P, Maeda Y, Hotary K, et al. Histone deacetylase inhibitor suberoylanilide hydroxamic acid reduces acute graft-versus-host disease and preserves graft-versus-leukemia effect. *Proc Natl Acad Sci USA.* 2004;101(11):3921-3926.
4. Reddy P, Sun Y, Toubai T, et al. Histone deacetylase inhibition modulates indoleamine 2,3-dioxygenase-dependent DC functions and regulates experimental graft-versus-host disease in mice. *J Clin Invest.* 2008;118(7):2562-2573.
5. Sun Y, Chin YE, Weisiger E, et al. Cutting edge: Negative regulation of dendritic cells through acetylation of the nonhistone protein STAT-3. *J Immunol.* 2009;182(10):5899-5903.
6. Tao R, de Zoeten EF, Ozkaynak E, et al. Deacetylase inhibition promotes the generation and function of regulatory T cells. *Nat Med.* 2007;13(11):1299-1307.
7. Choi SW, Braun T, Chang L, et al. Vorinostat plus tacrolimus and mycophenolate to prevent graft-versus-host disease after related-donor reduced-intensity conditioning allogeneic haemopoietic stem-cell transplantation: a phase 1/2 trial. *Lancet Oncol.* 2014;15(1):87-95.
8. Choi S, Reddy P. HDAC inhibition and graft *versus* host disease. *Mol Med.* 2011;17(5-6):404-416.
9. Kohler S, Thiel A. Life after the thymus: CD31+ and CD31- human naive CD4+ T-cell subsets. *Blood.* 2009;113(4):769-774.
10. Wieczorek G, Asemissen A, Model F, et al. Quantitative DNA methylation analysis of FOXP3 as a new method for counting regulatory T cells in peripheral blood and solid tissue. *Cancer Res.* 2009;69(2):599-608.
11. Kelly WK, O'Connor OA, Krug LM, et al. Phase I study of an oral histone deacetylase inhibitor, suberoylanilide hydroxamic acid, in patients with advanced cancer. *J Clin Oncol.* 2005;23(17):3923-3931.
12. Paczesny S, Krijanovski OI, Braun TM, et al. A biomarker panel for acute graft-versus-host disease. *Blood.* 2009;113(2):273-278.
13. Vander Lugt MT, Braun TM, Hanash S, et al. ST2 as a marker for risk of therapy-resistant graft-versus-host disease and death. *N Engl J Med.* 2013;369(6):529-539.
14. Leoni F, Zaliani A, Bertolini G, et al. The antitumor histone deacetylase inhibitor suberoylanilide hydroxamic acid exhibits antiinflammatory properties via suppression of cytokines. *Proc Natl Acad Sci USA.* 2002;99(5):2995-3000.
15. Grabiec AM, Krausz S, de Jager W, et al. Histone deacetylase inhibitors suppress inflammatory activation of rheumatoid arthritis patient synovial macrophages and tissue. *J Immunol.* 2010;184(5):2718-2728.
16. Rieger K, Loddenkemper C, Maul J, et al. Mucosal FOXP3+ regulatory T cells are numerically deficient in acute and chronic GvHD. *Blood.* 2006;107(4):1717-1723.
17. Magenau JM, Qin X, Tawara I, et al. Frequency of CD4(+)CD25(hi)FOXP3(+) regulatory T cells has diagnostic and prognostic value as a biomarker for acute graft-versus-host-disease. *Biol Blood Marrow Transplant.* 2010;16(7):907-914.
18. Matsuoka K, Koreth J, Kim HT, et al. Low-dose interleukin-2 therapy restores regulatory T cell homeostasis in patients with chronic graft-versus-host disease. *Sci Transl Med.* 2013;5(179):179ra43.
19. Edinger M, Hoffmann P, Ermann J, et al. CD4+CD25+ regulatory T cells preserve graft-versus-tumor activity while inhibiting graft-versus-host disease after bone marrow transplantation. *Nat Med.* 2003;9(9):1144-1150.
20. Akimova T, Beier UH, Liu Y, Wang L, Hancock WW. Histone/protein deacetylases and T-cell immune responses. *Blood.* 2012;119(11):2443-2451.
21. Akimova T, Ge G, Golovina T, et al. Histone/protein deacetylase inhibitors increase suppressive functions of human FOXP3+ Tregs. *Clin Immunol.* 2010;136(3):348-363.
22. Lucas JL, Mirshahpanah P, Haas-Stapleton E, Asadullah K, Zollner TM, Numerof RP. Induction of Foxp3+ regulatory T cells with histone deacetylase inhibitors. *Cell Immunol.* 2009;257(1-2):97-104.
23. Fontenot JD, Gavin MA, Rudensky AY. Foxp3 programs the development and function of CD4+CD25+ regulatory T cells. *Nat Immunol.* 2003;4(4):330-336.
24. Huehn J, Polansky JK, Hamann A. Epigenetic control of FOXP3 expression: the key to a stable regulatory T-cell lineage? *Nat Rev Immunol.* 2009;9(2):83-89.
25. Zheng Y, Josefowicz S, Chaudhry A, Peng XP, Forbush K, Rudensky AY. Role of conserved non-coding DNA elements in the Foxp3 gene in regulatory T-cell fate. *Nature.* 2010;463(7282):808-812.
26. Yuan ZL, Guan YJ, Chatterjee D, Chin YE. Stat3 dimerization regulated by reversible acetylation of a single lysine residue. *Science.* 2005;307(5707):269-273.
27. Mellor AL, Munn DH. IDO expression by dendritic cells: tolerance and tryptophan catabolism. *Nat Rev Immunol.* 2004;4(10):762-774.
28. Mestas J, Hughes CC. Of mice and not men: differences between mouse and human immunology. *J Immunol.* 2004;172(5):2731-2738.

OPEN ACCESS Freely available online

PLOS | ONE

Interleukin-17 Induces an Atypical M2-Like Macrophage Subpopulation That Regulates Intestinal Inflammation

Kenichiro Nishikawa[1], Naohiro Seo[2], Mie Torii[3¤], Nei Ma[4], Daisuke Muraoka[2], Isao Tawara[1], Masahiro Masuya[1], Kyosuke Tanaka[5], Yoshiyuki Takei[5], Hiroshi Shiku[2], Naoyuki Katayama[1☯], Takuma Kato[3*☯]

1 Department of Hematology and Oncology, Mie University Graduate School of Medicine, Tsu, Mie, Japan, **2** Department of Immuno-Gene Therapy, Mie University Graduate School of Medicine, Tsu, Mie, Japan, **3** Department of Cellular and Molecular Immunology, Mie University Graduate School of Medicine, Tsu, Mie, Japan, **4** Faculty of Health Science, Suzuka University of Medical Science, Suzuka, Mie, Japan, **5** Gastroenterology and Hepatology, Mie University Graduate School of Medicine, Tsu, Mie, Japan

Abstract

Interleukin 17 (IL-17) is a pleiotropic cytokine that acts on both immune and non-immune cells and is generally implicated in inflammatory and autoimmune diseases. Although IL-17 as well as their source, mainly but not limited to Th17 cells, is also abundant in the inflamed intestine, the role of IL-17 in inflammatory bowel disease remains controversial. In the present study, by using IL-17 knockout (KO) mice, we investigated the role of IL-17 in colitis, with special focus on the macrophage subpopulations. Here we show that IL-17KO mice had increased susceptibility to DSS-induced colitis which was associated with decrease in expression of mRNAs implicated in M2 and/or wound healing macrophages, such as IL-10, IL-1 receptor antagonist, arginase 1, cyclooxygenase 2, and indoleamine 2,3-dioxygenase. Lamina propria leukocytes from inflamed colon of IL-17KO mice contained fewer $CD11b^{+}Ly6C^{+}$MHC Class II^{+} macrophages, which were derived, at least partly, from blood monocytes, as compared to those of WT mice. FACS-purified $CD11b^{+}$ cells from WT mice, which were more abundant in $Ly6C^{+}$MHC Class II^{+} cells, expressed increased levels of genes associated M2/wound healing macrophages and also M1/proinflammatory macrophages. Depletion of this population by topical administration of clodronate-liposome in the colon of WT mice resulted in the exacerbation of colitis. These results demonstrate that IL-17 confers protection against the development of severe colitis through the induction of an atypical M2-like macrophage subpopulation. Our findings reveal a previously unappreciated mechanism by which IL-17 exerts a protective function in colitis.

Citation: Nishikawa K, Seo N, Torii M, Ma N, Muraoka D, et al. (2014) Interleukin-17 Induces an Atypical M2-Like Macrophage Subpopulation That Regulates Intestinal Inflammation. PLoS ONE 9(9): e108494. doi:10.1371/journal.pone.0108494

Editor: Markus M. Heimesaat, Charité, Campus Benjamin Franklin, Germany

Received June 27, 2014; **Accepted** August 21, 2014; **Published** September 25, 2014

Data Availability: The authors confirm that all data underlying the findings are fully available without restriction. All relevant data are within the paper and its Supporting Information files.

Funding: This study was supported in part by a Grant-in-Aid for Scientific Research from Japan Society for the Promotion of Science (25670553) to Dr. Takuma Kato. The funders had no role in study design, data collection and analysis, decision to publish, or preparation of the manuscript.

Competing Interests: Co-author Dr. Hiroshi Shiku has served as an editor for this journal and is still currently in that role. The authors confirm that this does not alter their adherence to PLOS ONE Editorial policies and criteria.

* Email: katotaku@doc.medic.mie-u.ac.jp

☯ These authors contributed equally to this work.

¤ Current address: Kyoto University Center for the Promotion of Interdisciplinary Education and Research, Kyoto, Japan

Introduction

Inflammatory bowel disease (IBD) including ulcerative colitis (UC) and Crohn's disease (CD) is a chronic inflammatory disease with recurring relapses and remissions in the lower gastrointestinal tract [1,2]. Genetic, environmental factors and their interrelationships which trigger an overactive adaptive immune response to intestinal bacterial flora have been considered to play key roles in the pathogenesis of IBD. More recent evidence suggests that defects in mucosal innate immune functions may also be involved in the etiology of IBD. However the exact pathomechanisms of the disease are still not fully elucidated.

IL-17, a signature cytokine of Th17 cells, is a pleiotropic cytokine with a primarily proinflammatory function that induces the production of other downstream inflammatory cytokines and chemokines [3]. IL-17 is found in abundance in the sera and affected tissues of various inflammatory and autoimmune diseases such as rheumatoid arthritis, multiple sclerosis, systemic lupus erythematosus psoriasis, and asthma and is well documented for its role in the pathogenesis of these diseases. IL-17 as well as their source, mainly but not limited to Th17 cells, is also found in the inflamed intestine in both animal models and humans [4,5], but the role of IL-17 in IBD remains controversial [6,7]. In models of both acute and chronic intestinal inflammation where mice were administered with trinitrobenzene sulfonic acid or infected with *Helicobacter hepaticus*, respectively, IL-17 showed a pathogenic role [8,9]. Likewise, antibody mediated neutralization of IL-17 in mice bearing a conditional deletion of Stat3 in $Foxp3^{+}$ T cells ameliorated the spontaneous colitis developed in these mice [10]. On the other hand, in a T-cell transfer colitis model, transfer of IL-$17^{-/-}$ T cells induced more severe colitis in $Rag^{-/-}$ mice [11]. In a dextran sulfate sodium (DSS)-induced colitis model, IL-17 has

been shown to exert pro- [12] and anti-[13,14] colitogenic activities, adding an additional layer of complexity.

These contradictory results regarding pathogenic versus protective roles of IL-17 mentioned above led us to re-examine whether IL-17 exerts protective function in a DSS-induced colitis model, focusing on the phenotypic and functional differences between macrophages in inflamed colon of WT and IL-17KO mice. Our results demonstrate that $CD11b^+Ly6C^+$MHC Class II^+ macrophages were reduced in the inflamed colon of IL-17KO mice that accompanied the development of more severe colitis as compared to WT mice. Depletion of $CD11b^+Ly6C^+$MHC Class II^+ macrophages in colon of WT mice resulted in more severe colitis. In vivo transfer experiments indicate that IL-17 promotes monocyte differentiation into M2-like macrophages. These results indicate that IL-17 protects from the development of DSS-induced colonic inflammation likely by promoting induction of unique macrophage subpopulation with anti-inflammatory and/or tissue repair functions.

Materials and Methods

Mice

C57BL/6 mice, C57BL/6 (CD45.1) congeneic mice and IL-17A deficient (IL-17KO) mice (C57BL/6 background) [15] were fed a standard diet, housed under specific pathogen free conditions and used at 5–8 weeks of age. All animal experiments were conducted under protocols approved by the Animal Care and Use Committee of Mie University Life Science Center.

Induction of colitis

Colitis was induced by 1.5% DSS (MW: 36,000–50,000, MP Biomedicals) dissolved in drinking water for 7 days followed by water alone. The body weight change was monitored daily up to 15 days. Healthy control animals received water only. In some experiments, DSS colitis was induced in mice adoptively transferred with monocytes or mice treated with clodronate liposomes. Briefly, monocytes (7×10^6 cells) isolated from bone marrow were transferred via tail vein into a group of mice a day before start of DSS treatment. Another group of mice were injected with 100 µl of clodronate liposomes or control liposomes (FormuMax Scientific Inc.) intrarectally using a feeding needle on days −1, 1, 3, and 5 of DSS administration.

Assay for intestinal permeability

To evaluate epithelial barrier function, intestinal permeability was assessed by administration of FITC-dextran as described [16]. Briefly, DSS treated mice were given FITC-dextran (MW: 4,000, Sigma-Aldrich, 40 mg/100 g of body weigh) by oral gavage 4 h before killing. The amount of FITC-dextran in serum was measured on spectrophotometer (Molecular Devices).

Isolation of colonic lamina propria leukocytes

Colonic lamina propria lymphocytes were collected from colons as described [17] with some modifications. Briefly, colons were resected and flushed with PBS to remove luminal contents. Colons were then opened longitudinally and cut into 0.5 cm pieces. The colonic pieces were incubated with HBSS without Ca^{2+} and Mg^{2+} containing 2.5% FCS, 1 mM DTT (Wako Pure Chemical Industries, Ltd. Japan), and 1% Penicillin-Streptomycin-Glutamine (Gibco) by shaking (200 rpm) at 37°C for 15 min to remove mucus. Subsequently, epithelial cells were removed through incubation with HBSS containing 2.5% FCS, 1mM EDTA, and 1% Penicillin-Streptomycin-Glutamine by shaking (200 rpm) at 37°C for 30 min. The colonic pieces were then digested in HBSS containing 2.5% FCS, 1.5 mg/ml Collagenase VIII (Sigma-Aldrich), and 0.1 mg/ml DNase I (Worthington Biochemical Corporation) by shaking (200 rpm) at 37°C for 30 min. Resultant cell suspensions were passed sequentially through cell strainers (100 µm), resuspended in 40% Percoll (GE Healthcare) and layered over an 75% Percoll prior to centrifugation at 2,500 rpm for 20 min. Cells from 40%/75% interface were collected, washed with HBSS for three times and used for experiments.

Isolation of monocytes

Monocytes were isolated from bone marrow with EasySep mouse monocyte enrichment kit (StemCell Technologies, Vancouver, CA), according to the manufacturer's instructions. Briefly, bone marrow cells from femora and tibiae were labeled with a cocktail of biotinylated antibodies against a panel of antigens expressed on T, B, NK, DCs, progenitor cells and granulocytes, followed by anti-biotin microbeads. Unlabeled monocytes were sorted magnetically by negative selection. Monocyte population contained more than 82% $CD11b^+Ly6C^+$ cells and less than 8% $Ly6G^+$ cells, and used for in vivo transfer experiments.

Flow cytometry

Colonic LP cells and monocytes were incubated with anti-CD16/32 (24G2; eBioscience) to block non-specific FcR followed by cell surface staining with corresponding mixture of fluorescently labeled mAbs. 7AAD (BD Pharmingen) was used to exclude nonviable cells. The following antibodies conjugated with FITC, PE, APC, V450, or APC/Cy7 were used for flow cytometry: anti-CD45.2 (104), anti-CD45.1 (A20), anti-I-Ab (AF6-120.1), anti-Ly6C (HK1.4), anti-F4/80 (BM8), anti-Ly6G (IA8), anti-CD206 (C068C2), anti-CD64 (X54-5/7.1), anti-CD127 (A7R34), anti-TCRγ/δ (GL3) (all from BioLegend), CD36 (NO. 72-1), anti-CCR9 (CW-1.2), anti-CCR7 (4B12), anti-CD11c (N418), anti-CD4 (RM4-5) (all from eBioscience), anti-CD11b (M1/70), Sca-1 (D7) (BD Bioscience), anti-CCR2 (475301) (R&D systems). PE-Rat IgG2a (eBR2a; eBioscience) and APC/Cy7-RatIgG2a (RTK 2758; BioLegend) were used as isotype matched control Abs. Data were acquired on a FACScant II (BD) and processed by using FlowJo software (Tree Star) with appropriate isotype controls to determine gating.

Gene expression analysis

Total RNA was extracted from distal colon segments or purified cells with Trizol reagent (Invitrogen) and reverse transcribed into cDNA as described [18]. Realtime RT-PCR was performed by using FastStart Universal SYBR Green Master (Roche Diagnostics) according to the manufacturer's instruction. Expression of target mRNA were normalized to the expression of β-actin mRNA for generation of ΔCt values, and relative mRNA expression was quantified with the ΔΔCt method [19]. Primer sequences for these reactions were designed by using Primer Express software Version 3 (Applied Biosystems) and provided in the Table S1.

Histology

Distal colon tissue was fixed in 10% paraformaldehyde and embedded in paraffin blocks. Five micrometer sections were stained with hematoxylin and eosin.

Statistics

Statistic analyses were performed with IBM SPSS Statistics Software Version 19 (IBM). Differences between two groups were compared using the two-tailed Student's t-test and those among multiple groups were compared using the Kruskal-Wallis with

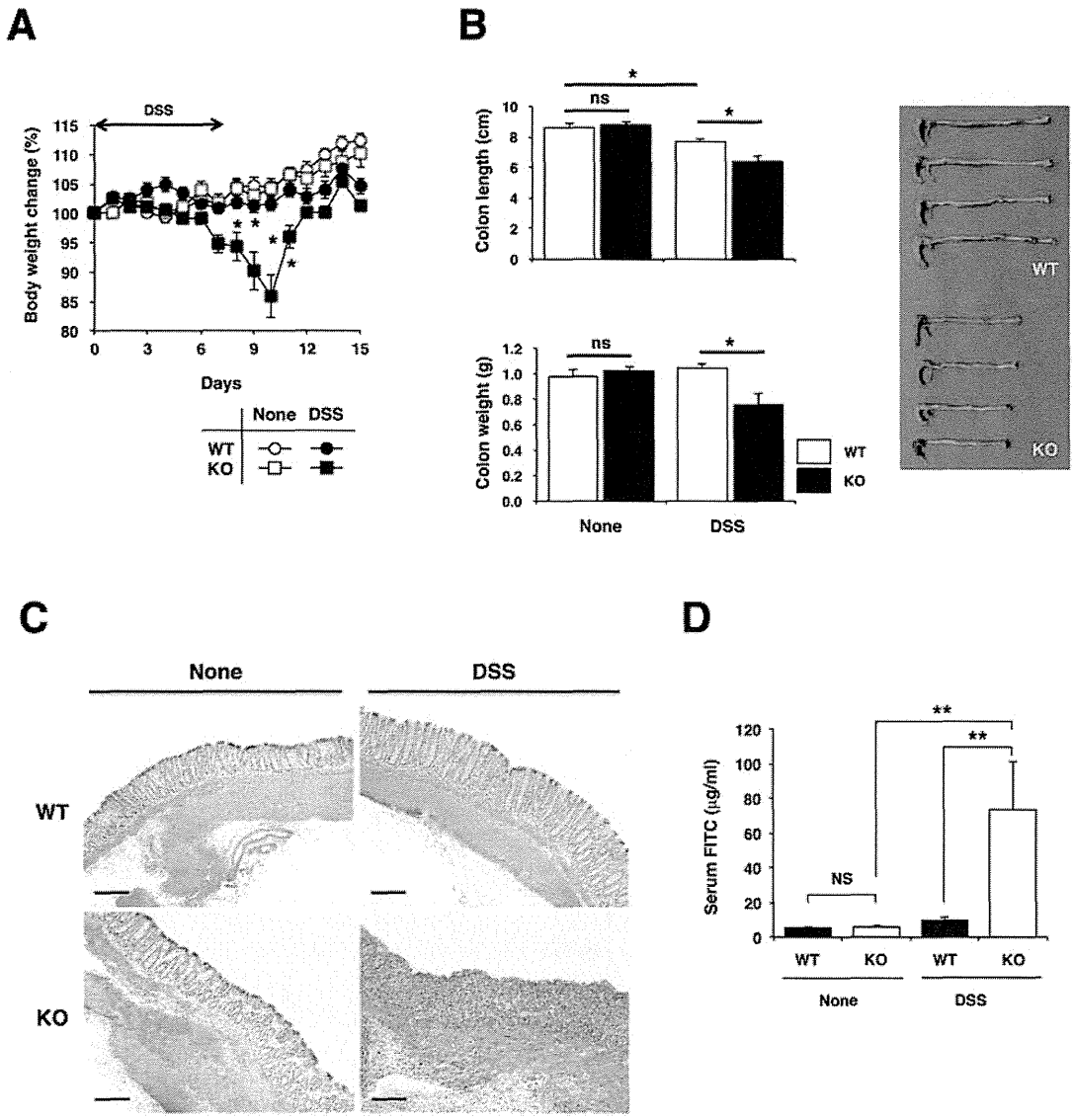

Figure 1. IL-17 deficient mice exhibit more severe acute colitis following DSS administration. IL-17KO mice and WT controls were given 1.5% DSS in drinking water or water alone for 7 days followed by consumption of water alone. Colitis severity was assessed by weight loss (A), colon length (day 10) (B) and H&E histology (day 0 and 10) (Calibration bar = 200 μm) (C). Colon barrier permeability was assessed on day 10 by detection of FITC-dextran serum (D). The results are expressed as mean values ± SEM for each geneotype in A (n = 5–6), B (n = 10), C (n = 2), and D (n = 5). *p<0.05; **p<0.01.
doi:10.1371/journal.pone.0108494.g001

Bonferroni post hoc' test. A p value of <0.05 was considered significant. All experiments were performed more than two times. Data are presented as mean ± SEM.

Results

IL-17-deficient mice exhibit more severe acute colitis following DSS administration

To reassess the role of IL-17 in DSS-induced colitis, we administered 1.5% DSS in drinking water to age- and sex-matched IL-17KO and WT mice for 7 days followed by water consumption alone with untreated mice serving as controls. At a steady state, both genotypes displayed no gross signs of colitis such as growth retardation, weight loss or diarrhea. Although ingestion of DSS is known to cause intestinal inflammation in WT mice as a result of disruption of the gut epithelial barrier, this dose of DSS did not induce marked weight loss in WT mice (Figure 1A). By sharp contrast, IL-17KO mice experienced significant weight loss starting at day 7, reaching a maximum reduction (15%) on day 10, followed by a recovery that reached a pretreatment level at day 5 after DSS withdrawal. In addition, IL-17KO mice showed a more decrease in colon length and weight by day 10 as compared to WT mice (Figure 1B). Histological analysis also revealed aggravated colonic inflammation as evidenced by edema, high degree of ulcerations and overt inflammatory infiltrate in both mucosa and submucosa, and mucosal thickening accompanied by destruction of epithelium in IL-17KO mice (Figure 1C). Concomitant with these findings, epithelial barrier function in IL-17KO mice was